

Horseradish Peroxidase-catalyzed Oligomerization of Ferulic Acid on a Template of a Tyrosine-containing Tripeptide*

Received for publication, February 19, 2002, and in revised form, March 27, 2002
Published, JBC Papers in Press, March 29, 2002, DOI 10.1074/jbc.M201679200

Gideon Oudgenoeg,^{a,b,c} Eef Dirksen,^{b,d} Steen Ingemann,^e Riet Hilhorst,^{a,b,f}
Harry Gruppen,^{a,c} Carmen G. Boeriu,^g Sander R. Piersma,^{a,h,i} Willem J. H. van Berkel,^{a,b}
Colja Laane,^{b,j} and Alphons G. J. Voragen^{a,c,k}

From the ^aCentre for Protein Technology TNO-WU, Bomenweg 2, 6700 EV Wageningen, ^bLaboratory of Biochemistry, Department of Agrotechnology and Food Sciences, Wageningen University, Dreijenlaan 3, 6703 HA Wageningen, ^cLaboratory of Food Chemistry, Department of Agrotechnology and Food Sciences, Bomenweg 2, 6700 EV, Wageningen University, Wageningen, ^eSwammerdam Institute for Life Sciences, Faculty of Science, University of Amsterdam, Nieuwe Achtergracht 166, 1018 WV Amsterdam, ^gATO, Bornsesteeg 59, 6708 PD, Wageningen, and ^hTNO Food and Nutrition Research, Utrechtseweg 48, 3700 AJ Zeist, The Netherlands

Ferulic acid (FA) is an abundantly present phenolic constituent of plant cell walls. Kinetically controlled incubation of FA and the tripeptide Gly-Tyr-Gly (GYG) with horseradish peroxidase and H₂O₂ yielded a range of new cross-linked products. Two predominant series of hetero-oligomers of FA linked by dehydrogenation to the peptidyl tyrosine were characterized by electrospray ionization (tandem) mass spectrometry. One series comprises GYG coupled with 4–7 FA moieties linked by dehydrogenation, of which one is decarboxylated. In the second series 4–9 FA moieties linked by dehydrogenation, of which two are decarboxylated, are coupled to the tripeptide. A third series comprises three hetero-oligomers in which the peptidyl tyrosine is linked to 1–3 FA moieties of which none is decarboxylated. Two mechanisms for the formation of the FA-Tyr oligomers that result from the dualistic, concentration-dependent chemistry of FA and their possible role in the regulation of plant cell wall tissue growth are presented.

Plant peroxidases (donor: hydrogen-peroxide oxidoreductases, EC 1.11.1.7) have often been suggested to be involved in the biosynthesis of complex plant cell wall macromolecules constituting lignin and suberin tissues. Lignins are located in the primary and secondary walls of specific plant cells and are synthesized for mechanical strength, defense, and water transport in terrestrial vascular plants. The temporal and spatial correlation between lignin synthesis and peroxidase catalysis has been suggested based on studies of the enzyme, the hydroxycinnamic acid substrates, and the hydrogen peroxide co-substrate *in vivo*. In lignin tissues of transgenic plants, the

Arabidopsis ATP A2 peroxidase promoter directs GUS reporter gene expression, indicating involvement of the peroxidase in the assembly of the lignin polymer (1). After administration of the reducing substrate [¹³C]ferulic acid to wheat cell walls for extended duration, elevated levels of ferulic acid in the lignin-like tissues were revealed by *in situ* solid state ¹³C NMR (2). In *Pinus taeda* cell suspension cultures, lignin synthesis is correlated with the generation of the oxidizing co-substrate H₂O₂ (3). Suberin provides a physical barrier to moisture loss in plants as well as a defensive shield against pathogens. In the potato, a H₂O₂-generating system with NAD(P)H-dependent oxidase-like properties is temporarily associated with suberin synthesis (4), and the polyaromatic domain of suberins in wound-healing potato (*Solanum tuberosum*) tubers is constituted of polymers derived from hydroxycinnamic acid (5).

Ferulic acid (FA,¹ 3-(4-hydroxy-3-methoxyphenyl)-2-propenoic acid), a hydroxycinnamic acid that is often found to be esterified to plant cell wall polysaccharides (6, 7) is a good substrate for most plant peroxidases. The x-ray structure of horseradish peroxidase C (HRP C) in complex with FA (8) provides molecular insight into the initial abstraction of the hydroxyl hydrogen via one-electron oxidation and subsequent deprotonation of the cation radical, resulting in the FA free radical. Dehydrodimers of FA stemming from radical combination have been identified in plant cell walls (9–13). *In vitro*, similar FA dehydrodimers have been identified after incubation of peroxidase with either free FA or FA esterified to pectins and arabinoxylans (14). Recently, it was reported that in incubations with lignin peroxidase, higher polymers of ferulic acid are formed, and the structures of two dehydrotrimers were assigned by ¹H NMR (15).

Tyrosine, both as free amino acid and in peptides or proteins, is also a substrate for many plant peroxidases. After one-electron oxidation and subsequent deprotonation, a tyrosine radical species is formed that can combine with another tyrosine radical at either the phenolic oxygen or at one of the *ortho* positions of the aromatic ring (16). Dityrosines and higher oligomers resulting from peroxidase-mediated combination of tyrosine radicals have been characterized for tyrosine-containing peptides (17–19). The *in vivo* occurrence of dityrosines in proteins was first demonstrated in insect cuticle (20). Upon

* This research was supported by the Ministry of Economic Affairs of The Netherlands through the program Innovatief Onderzoek Programma-Industrial Proteins and by AVEBE, DMV-International, Hercules, Quest International, and Unilever. The costs of publication of this article were defrayed in part by the payment of page charges. This article must therefore be hereby marked "advertisement" in accordance with 18 U.S.C. Section 1734 solely to indicate this fact.

^a Present address: Dept. of Biomolecular Mass Spectrometry, Utrecht University, Sorbonnelaan 16, 3584 CA Utrecht, The Netherlands.

^f Present address: Pamgene BV, P. O. Box 1345, 5200 BJ, Hertogenbosch, The Netherlands.

^g Present address: FOM institute for Atomic and Molecular Physics, Amsterdam, The Netherlands.

^h Present address: DSM Food Specialties, A. Fleminglaan 1, 2600 MA Delft, The Netherlands.

^k To whom correspondence should be addressed. Tel.: 31-317484469; Fax: 31-317484893; E-mail: Fons.voragen@chem.fdsi.wag-ur.nl.

¹ The abbreviations used are: FA, ferulic acid; HRP, horseradish peroxidase; HPLC, high pressure liquid chromatography; MS, mass spectrometry; MS², tandem mass spectrometry; MS³, subsequent CID after spectrometry MS; CID, collision-induced dissociation.

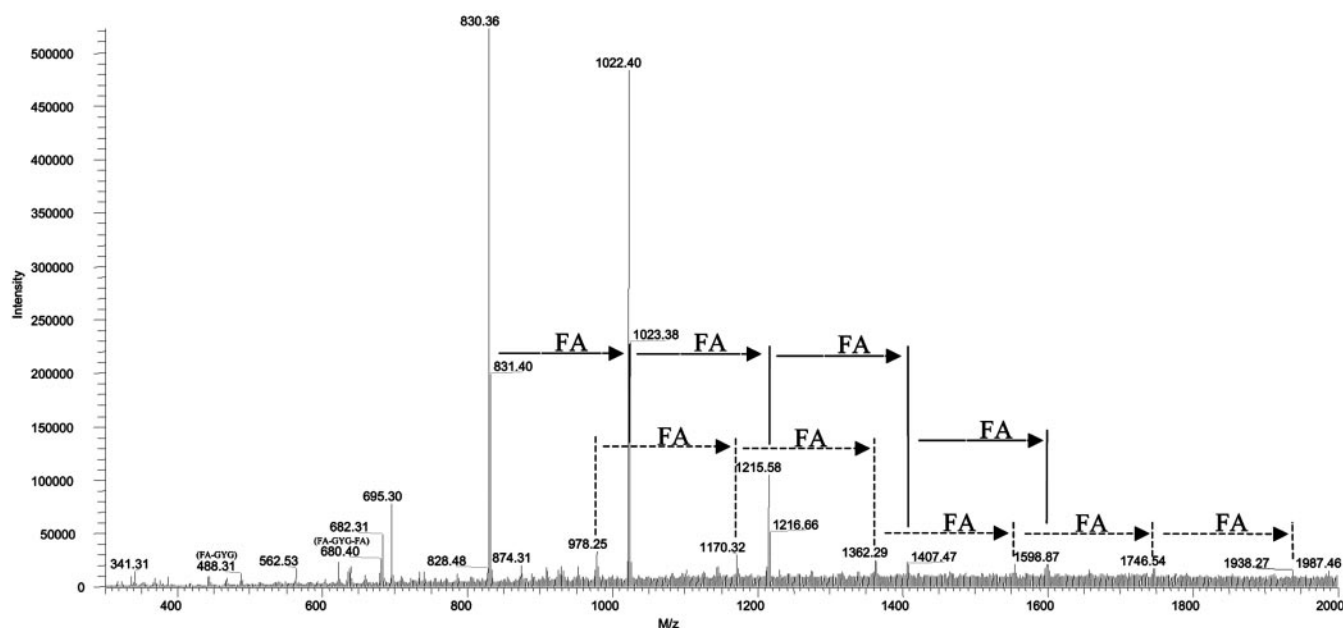


FIG. 1. Nano-electrospray mass spectrum of the redissolved incubation mixture.

elicitor and wound induction of bean and soybean cell walls, a rapid oxidative cross-linking of the (hydroxy)proline-rich glycoproteins was demonstrated (21). These structural proteins contain highly repetitive peptide sequences, among which the tyrosine-containing Val-Tyr-Lys-Pro-Pro pentapeptide. *In vitro*, dityrosines stemming from peroxidase catalysis in proteins were demonstrated in soluble collagens and in wheat prolamine (22).

Because both FA and tyrosine are subject to peroxidase-mediated oligomerization, we rationalized that hetero-coupling of these substrates should be feasible (19). Such peroxidase-mediated hetero-coupling could provide an explanation for the occurrence of protein-carbohydrate complexes in plant cell walls and the incorporation of FA and other hydroxycinnamic derivatives into lignin and suberin tissues on a protein template. From an earlier study with the tripeptide Gly-Tyr-Gly (GYG) and FA, we established conditions that resulted in covalent linkage of FA and the peptidyl tyrosine (19). Evidence was provided for the peroxidase-mediated formation of GYG oligomers linked by dehydrogenation, ranging from dimers to pentamers that are oxidatively cross-linked to either one or two molecules of FA (19). In the present study we have further explored the mechanism of hetero-adduct formation of GYG and FA. Complementary to the aforementioned studies (2, 3, 5, 9, 10, 13) in which the constituting precursor moieties in plant cell wall tissue were deduced from the *in vivo* synthesized biopolymer, we now present the *in vitro* synthesis of the biopolymer by HRP and H₂O₂ from the hypothesized FA precursor on a tyrosine template.

MATERIALS AND METHODS

Glycine-tyrosine-glycine (GYG) was obtained from Bachem, Bubendorf, Switzerland. HRP (type VI-A) and FA were obtained from Sigma. Hydrogen peroxide (30% v/v) was obtained from Merck. All other chemicals were of analytical grade.

Incubation—Solutions of 12.44 mM ferulic acid and 12.44 mM H₂O₂ (kept on ice) in 50 mM sodium phosphate, pH 8.0, containing 10% (v/v) acetonitrile were continuously and simultaneously added to the incubation mixture using two peristaltic pumps (LKB Bromma 2232 Microperpex S). The incubation mixture, thermostatted at 20 °C, contained 25 mM GYG and 1.25 mg of HRP in an initial volume of 10 ml of 50 mM sodium phosphate, pH 8.0. 20 ml of the FA solution and 20 ml of the H₂O₂ solution were added over a 15-min period. After another 10 min of incubation, the reaction mixture was frozen in liquid nitrogen,

freeze-dried, and stored at 4 °C until analysis.

HPLC-MS—For liquid chromatography-MS analysis, 20 μ l of the reaction mixture (10 mg of lyophilisate redissolved in 100 μ l of MilliQ water) was separated on a 150 \times 2.1-mm Alltima C18 column (Alltech, Breda, The Netherlands) running in 0.03% (v/v) trifluoroacetic acid in water at a flow rate of 0.2 ml/min. Elution was performed with a linear gradient of 0–40% acetonitrile in 0.03% (v/v) trifluoroacetic acid in water over a 45-min period.

Mass spectrometric analysis was performed with a LCQ ion trap (Finnigan MAT 95, San José, CA) with the use of electrospray ionization and detection in the positive ion mode. The capillary spray voltage was 2.5 kV, and the capillary temperature was 200 °C. The instrument was controlled by Xcalibur software. The accuracy of the mass determinations is ± 0.5 Da. After a full MS scan, ions with a mass to charge (m/z) ratio within 10 m/z units of the most abundant ion were selected and subjected to collision-induced dissociation (CID, MS²). The five most abundant product ions resulting from the first stage of CID were fragmented further by a second stage of CID (MS³). For nanospray MS, 10 μ l of the redissolved reaction mixture was diluted with acetonitrile (1:1) and loaded in a conductive metal-coated (coating 3AP) nanospray tip (2-mm internal diameter) (NewObjective, Woburn, MA) using a Gelloader pipette tip (Eppendorf). Nanospray conditions used were 25 units of nitrogen backing pressure and 1.2-kV ionization spray voltage, and the heated desolvation capillary was held at 200 °C. 500 scans detected in the positive-ion mode were averaged.

RESULTS

After freeze-drying the incubation mixture, a yellow/orange powder was obtained. Nano-electrospray MS of the redissolved lyophilisate revealed two dominant series of products (Fig. 1). The most abundant ion series starts at m/z 830.36 and proceeds with average m/z increases of 192 to ions with apparent m/z values of 1022.40, 1215.58, 1407.47, and 1598.87. The other series starts at m/z 978.25 and proceeds with average m/z increases of 192 to ions with apparent m/z values of 1170.32, 1362.29, 1554.42, 1746.54, and 1938.27. The difference of 192 between the ions in both series corresponds to FA linked by dehydrogenation. According to the total ion current after reverse phase HPLC of the redissolved incubation mixture, species with m/z 829.8, 1021.9, and 978.0 are the three most abundant ions (Fig. 2a). Figs. 2, b–g, show the single ion chromatograms of the reverse phase HPLC elution of these and three other selected species with a m/z of 341.0, 1213.8, and 873.9 (mono-isotopic), respectively. All these species are singly charged, as apparent from the m/z difference of 1 between the first 3 ¹³C isotopes in the partial mass spectra obtained by

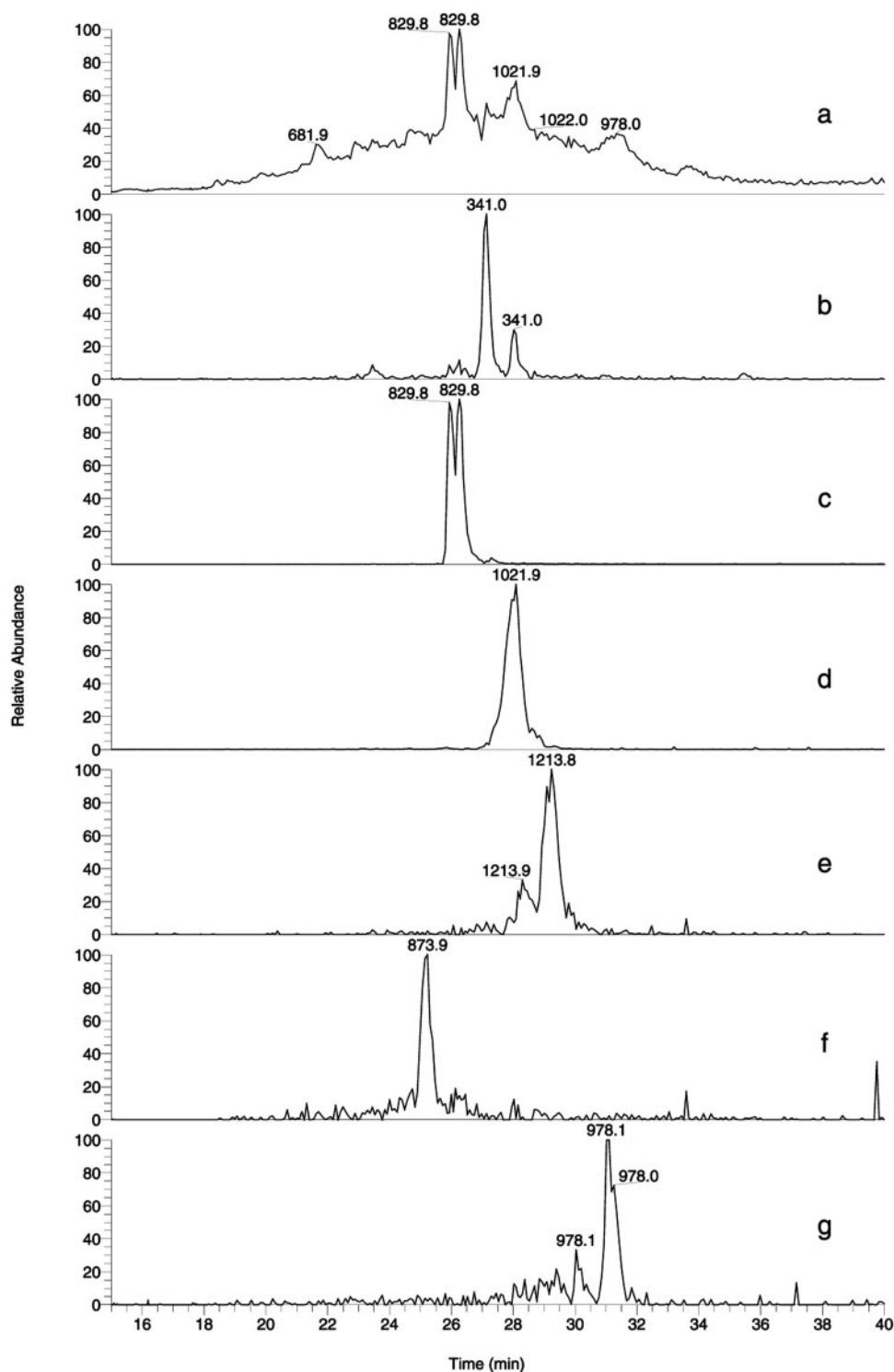


FIG. 2. Reverse phase-HPLC-MS chromatogram of the crude incubation mixture. *a*, total ion current. Single ion chromatograms of *m/z* species of 341.0 (*b*), 829.9 (*c*), 1021.9 (*d*), 1213.8 (*e*), 873.9 (*f*), and 978.1 (*g*).

selection of ions within 10 *m/z* units from the ion of interest (data not shown). Therefore, the molecular mass of the compounds is considered equal to the apparent *m/z* values.

The most abundant species is the ion with an apparent *m/z* value of 829.8 (mono-isotopic). The mass corresponds to a hetero-tetramer of 1 GYG linked by dehydrogenation to a decarboxylated trimer of FA. In the single ion chromatogram of this compound (Fig. 2, panel *c*), two main isomers, nearly base line-resolved, were detected. Upon collision-induced dissociation of the *m/z* 829.8 ions, positively charged product ions with

m/z 636.0 and 441.8 result (Fig. 3, panel *c*), stemming from consecutive loss of 2 FA moieties (194 Da each). The fragment ions with *m/z* 366.8 and 339.0 originate from further dissociation of the *m/z* 441.8 ion after consecutive loss of Gly and CO from the peptide moiety, resulting in the b2 and a2 ion of the modified tripeptide, as is proved by collision of the isolated *m/z* 441.8 ion during a second stage of CID (MS^3).

The second predominant ion, *m/z* 1021.9 (mono-isotopic), corresponds to dehydrogenation linkage of another FA moiety to the hetero-tetramer with a *m/z* of 829.8 and is assigned to a

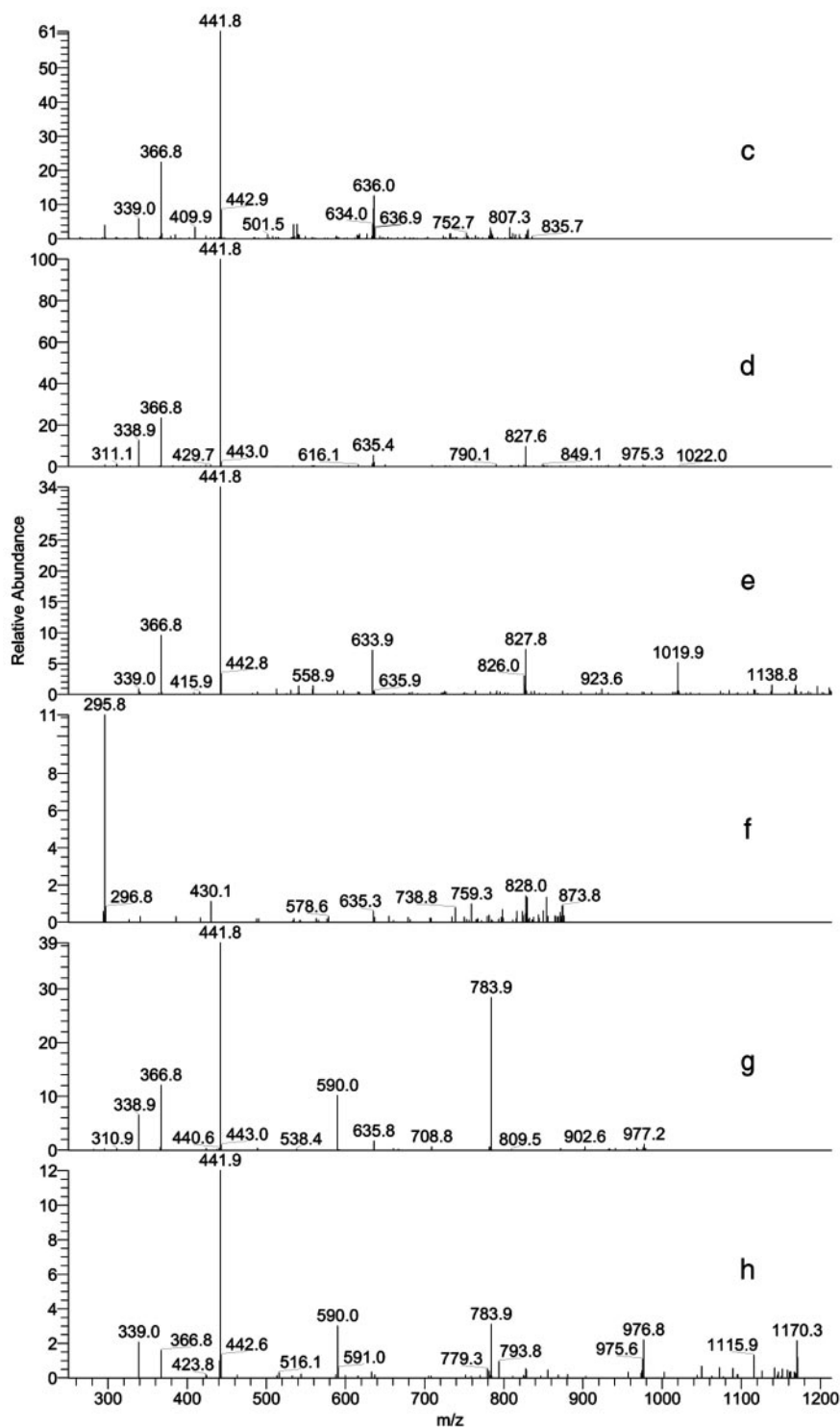


FIG. 3. Fragmentation spectra of CID (MS^2) of m/z species of 829.9 (c), 1021.9 (d), 1213.8 (e), 873.9 (f), 978.1 (g), and 1170.3 (h); for convenience, the letter designating each fragmentation spectrum corresponds to the letter indicating the concomitant single ion chromatogram in Fig. 2 and therefore starts at c.

hetero-pentamer of 1 GYG linked by dehydrogenation to 4 FA molecules, of which one is decarboxylated. In the single ion chromatogram of this compound, several co-eluting isomers were detected (Fig. 2, panel d). Upon CID of any of these m/z 1021.9 ions, positively charged product ions with m/z 827.6, 635.4, and 441.8 result (Fig. 3, panel d), stemming from consecutive losses of 3 FA moieties (194, 192, and 194 Da). A second stage of CID (MS^3) on both the isolated m/z 827.6 and isolated m/z 635.4 fragment ions results in the same m/z 441.8 fragment ion as resulted from CID of the hetero-tetramer, indicating the same structural element in the hetero-pentamer.

In the single ion chromatogram of the third consecutive

hetero-oligomer in this series of hetero-oligomers, m/z 1213.8, 1 minor isomer and 2 co-eluting major isomers were detected (Fig. 2, panel e). These are assigned to a hetero-hexamer of 1 GYG peptide linked by dehydrogenation to 5 FA, of which 1 is decarboxylated. Upon CID of any of these isomers, fragment ions with m/z 1019.9 (loss of one FA, 194 Da), m/z 827.8 (loss of second FA, 192 Da), m/z 635.9 (loss of third FA, 192 Da) and predominantly fragment ions of m/z 441.9, 366.8, and 339.0 result (Fig. 3, panel e). The three “fingerprint” ions again demonstrate a constituting moiety similar to that in the preceding compounds in this series.

One higher hetero-oligomer in this series was found (Fig. 1),

and this m/z 1407.3 species is assigned to a hetero-heptamer of 1 GYG and 6 FA, of which 1 is decarboxylated. CID of this ionized compound predominantly yielded the fragment ions with m/z 825.9 (loss of 3 FA moieties) and 441.8 (loss of 5 FA moieties) and is concluded to contain the same structural element. The full ion series with m/z values of 829.9, 1021.9, 1214.4, and 1405.8 are assigned to GYG-FA oligomers linked by dehydrogenation containing 3, 4, 5, or 6 FA moieties respectively, each containing the same structural element consisting of a covalent adduct of 1 GYG and decarboxylated FA. The base line-resolved-eluting m/z 341.0 species (Fig. 2, panel b) are assigned to isomeric decarboxylated dehydrodimers of FA.

The third predominant ion in the total ion current, m/z 978.1 (Fig. 2, panel a), is assigned to a hetero-pentamer of 1 GYG linked by dehydrogenation to 4 FA moieties, of which 2 are decarboxylated. Several minor isomers elute separated from two major isomers that co-elute (Fig. 2, panel g). CID of these isomers results in fragment ions with m/z 783.4 and 590.0 (Fig. 3, panel g), corresponding to the consecutive loss of two FA moieties (194 Da). Loss of a third, decarboxylated, FA (148 Da) leads to the main fingerprint fragment ion with m/z 441.8 and the other two fingerprint ions with m/z 366.8 and 339.0 (Fig. 3, panel g). Therefore the core structural element is concluded to be the same as for the single fold decarboxylated series of hetero-oligomers.

The second predominant product in this ion series, m/z 1170.3 (Fig. 1), corresponds to dehydrogenation linkage of another FA moiety to the 2-fold decarboxylated hetero-pentamer with m/z 978.1 and is assigned to a hetero-hexamer of 1 GYG linked by dehydrogenation to 5 FA molecules, of which 2 are decarboxylated. In the single ion chromatogram of this compound (data not shown), several co-eluting isomers were detected at a retention time similar to that of the m/z 978.1 species. Upon ESI and CID of any of these m/z 1170 species, positively charged ions with m/z 976.8, 783.9, 590.0, and 441.8 result (Fig. 3, panel h), originating from consecutive losses of 4 FA moieties (194, 193, 194, and 148). The full series of ions starting at m/z 978.3 (Fig. 1) are therefore assigned to hetero-oligomers of 1 GYG coupled by dehydrogenation with 4–9 FA moieties, of which 2 are decarboxylated.

The m/z 873.9 ion (Fig. 1 and the chromatogram in Fig. 2f) is assigned to a hetero-tetramer of 3 nondecarboxylated FA moieties and 1 GYG. This m/z value of this species corresponds to 2 FA molecules linked by dehydrogenation and 1 FA molecule not linked by dehydrogenation to GYG. CID of these ions (Fig. 3, panel f) results in different product ions as compared with the series of 1- and 2-fold decarboxylated hetero-oligomers, and the fingerprint ions from the former series are completely absent. This implies that the ion with a m/z of 873.9 cannot contain the m/z 441.9 moiety like the former series of hetero-oligomers. The main fragment ion is that with m/z 295.8, corresponding to the GYG ion after loss of the FA moieties. No higher hetero-oligomers containing exclusively nondecarboxylated FA moieties were found. However, two smaller nondecarboxylated hetero-oligomers, m/z 488 (hetero-dimer) and m/z 680 (hetero-trimer), were formed in minor amounts (Fig. 1). Interestingly, these compounds were main products in a previous incubation (19).

DISCUSSION

In this study it is shown that the kinetically controlled incubation of FA and GYG with peroxidase and H_2O_2 results in a complex range of (isomeric) products of different degrees of polymerization. Because isolation of these products for NMR characterization is not straightforward, mass spectrometry including a first and second stage of collision-induced dissociation was the method of choice to elucidate the range of products

and their compositional structural elements.

In both the series of 1-fold decarboxylated and the series of 2-fold decarboxylated hetero-oligomers the difference in mass between the compounds was always 192 Da, a mass difference expected for dehydrogenation linkage of FA to each preceding compound in a constitutive fashion. Unambiguous assignment of the ions of the compounds to the constituting moieties of the two series of hetero-oligomers is provided by CID. Upon CID of a hetero-oligomer, the covalent linkages in the proximity of the C-C bond that connects the four aromatic moieties A, B, C, and Tyr (Fig. 4, structure 5h e.g.) are most susceptible to fragmentation due to the high probability of the presence of the proton in this acetal-type structural moiety. After loss of two neutral FA moieties, the 441.9 fragment results (Fig. 4, structure 5h₄). Further fragmentation of this fragment (MS^3) resulted in the b₂ and a₂ ions (Fig. 4, structures 5h₆ and 5h₇) that further validates the assignment of the 441.9 fingerprint ion as GYG linked to the decarboxylated FA moiety. The presence of the fragment ion of 441.9 (Fig. 3, panels c, d, e, g, and h) in all MS^2 spectra of compounds of the one- or 2-fold decarboxylated hetero-oligomers and the fragments of 367 and 339 in the MS^3 spectrum of the parent mass 441.9 clearly indicates that the GYG peptide bound to the decarboxylated FA moiety (Fig. 4, all structures, ring C) is always one of the constituting moieties of at least 1 isomer of the 1- and 2-fold decarboxylated hetero-oligomers. Most of the other, isomeric hetero-tetramers (Fig. 6b, structures 5a–h) are unlikely to lead to the fingerprint fragment ions as outlined for isomer 5h in Fig. 4. However, these species may well contribute to the total ion current of the compound of interest but not participate in the fragmentation pattern of a co-eluting isomer.

In contrast to the 1- and 2-fold decarboxylated hetero-oligomers, the fragmentation of the 873.9 species (Fig. 3, panel f) does not lead to product ions corresponding to the m/z 441.9 structural element (Fig. 4, structure 5h₄). This nondecarboxylated hetero-oligomer results mainly in an m/z 295.8 product ion (Fig. 3, panel f), which corresponds to GYG with no decarboxylated FA moiety attached. This distinct product ion pattern was also found for nondecarboxylated FA-GYG-FA and FA-GYG in a previous study, where GYG was kept in excess over FA (19) during the incubation. Higher hetero-oligomers of this type were not found in those studies nor in the present one.

This discrepancy between the wide range of decarboxylated, further oligomerized hetero-oligomers and the limited range of nondecarboxylated, maximally tetrameric hetero-oligomers suggests two different mechanisms for the covalent attachment of FA to the tyrosine template. Under the conditions applied, the main route occurs via radical attack on the vinylic bond of the decarboxylated FA dimer (Fig. 5a, structures 2a and 2b), whereas the minor route proceeds via de- or nondehydrogenation addition of the non-decarboxylated monomeric FA radical. The main route deduced from the present data is supported by a recently proposed mechanism for the lignin peroxidase-catalyzed homo-trimerization of FA (15). This mechanism comprises an attack by a phenoxy-FA radical (Fig. 5a, structure 1a) on the vinylic bond of a decarboxylated FA dehydromer (Fig. 5, structures 2a and 2b). The initially formed trimeric FA radical species resulting from this attack (Fig. 5b, structures 3a–d) can be oxidized and, after deprotonation, result in a FA trimer, as was authenticated by one- and two-dimensional 1H NMR (15). Decarboxylated dehydrodimers of FA were also formed in the present HRP-mediated incubation of GYG with FA (Fig. 2, panel b).

Because GYG radicals are continuously present (Fig. 6a, structures 4a and 4b) in the hetero-incubation, as follows from the presence of GYG dimers (data not shown), two routes can

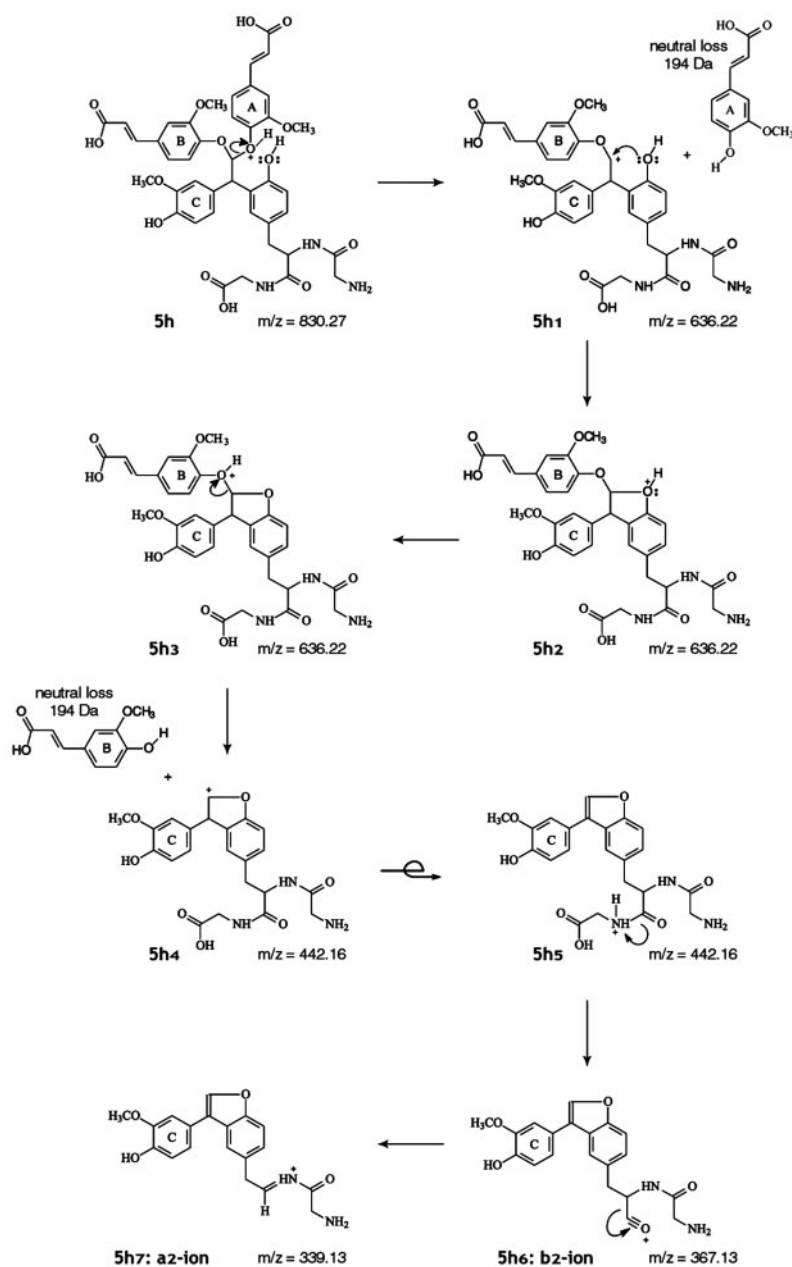


FIG. 4. Mechanism of collision-induced dissociation of hetero-tetramer 5h.

directly lead to a hetero-oligomer. Combination of the trimeric FA radical (Fig. 5b, structures 3a–d) with the peptidyl tyrosine radical of an oxidized GYG (Fig. 5a, structures 4a or 4b) results in a hetero-tetramer comprising 3 FA and 1 GYG (Fig. 6b, structures 5a–h). Attack of the GYG radical on the vinylic bond of the decarboxylated FA dimer and subsequent combination of the resulting hetero-trimeric radical with another FA radical also leads to the hetero-tetramer, whereas attack of the hetero-trimeric radical on another decarboxylated FA dimer leads to a 2-fold decarboxylated hetero-pentamer. These routes, both via decarboxylated FA dimers, appear to be important in the oligomerization to higher FA oligomers on the peptide since the higher hetero-oligomers always are 1- or 2-fold-decarboxylated. Any of the 1-fold decarboxylated hetero-tetramers (Fig. 6b, structures 5a–h) or 2-fold decarboxylated hetero-pentamers evolved from this reaction path still has several sites for further oligomerization to higher hetero-oligomers.

On the basis of the similar product pattern of polymerization of FA by either Lignin peroxidase or HRP, it was suggested that FA oligomerization is governed by radical chemistry

rather than enzyme specificity (15). These findings are in agreement with our data, which show that it is the chemistry of the enzymatically primarily formed radical products and especially the chemistry of the decarboxylated dehydrodimers of FA that leads to oligomerization. The GYG-FA hetero-oligomers found in the present study are clearly distinct from the ones found in a previous study (19). This shows that the type of oligomerization is strongly dependent on the substrate concentrations and kinetic control of the reaction.

Our present findings confirm the suggestion of Ward *et al.* (15) that the peroxidase-induced cross-linking of FA leads to higher oligomers than the trimers they identified by NMR. Furthermore, the attachment of higher oligomers of FA bound to a peptidyl tyrosine would supply a spatial basis for the covalent anchoring of easy diffusible small phenols on a tyrosine template in a plant cell wall protein and supports the often hypothesized template-guided *in situ* polymerization process of lignin (23–25). During growth or stress, increased levels of FA in the plant can result in differentiation of the type of tissue formed in a similar fashion as the kinetically and stoichiomet-

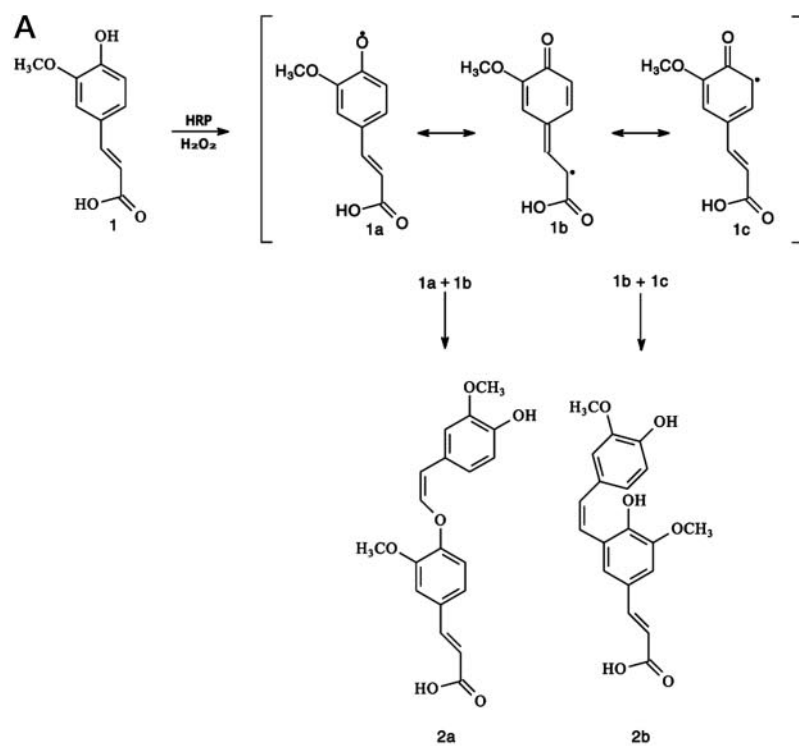
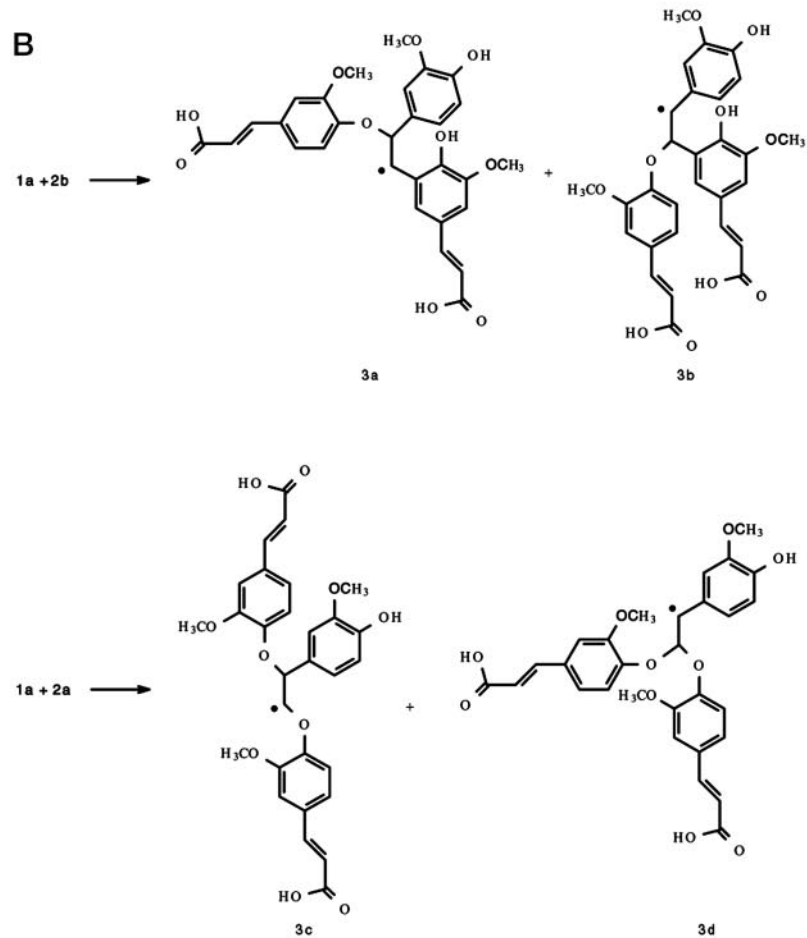


FIG. 5. HRP-catalyzed oxidation of FA, combination of monomeric FA radicals to decarboxylated dehydrodimers, and attack of monomeric FA radicals on the vinylic bond of the decarboxylated dehydrodimers leading to trimeric FA radicals.



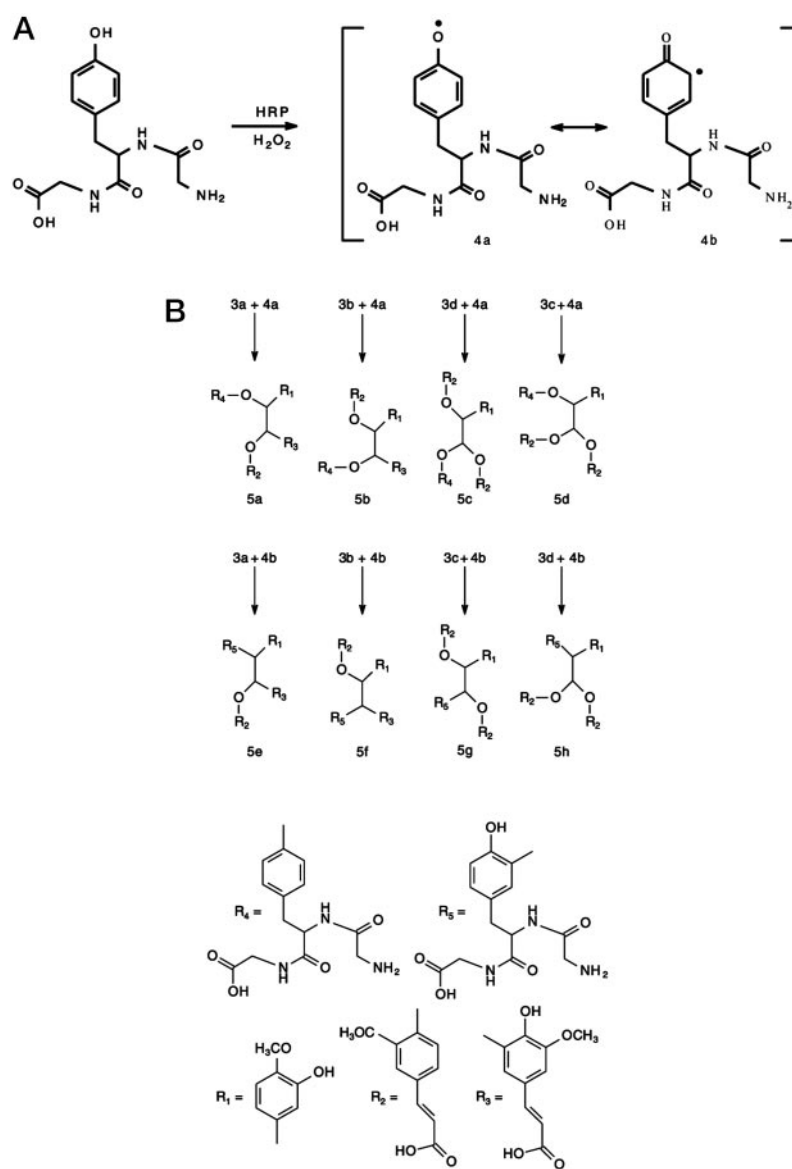


FIG. 6. *a*, HRP-catalyzed oxidation of GYG. *b*, eight possible hetero-tetrameric radicals resulting from radical combination of two isomeric GYG radicals and four isomeric trimeric FA-radicals.

rically controlled polymerization of FA described in this paper. The phenolic moiety enables oxidation of the molecule as a trigger for oxidative polymerization, whereas the vinylic moiety stabilizes the radical and allows further polymerization after decarboxylative dimerization.

Just as the peptide oligomers in a previous study always appeared to be blocked for further oligomerization by two non-decarboxylated FA molecules linked by dehydrogenation to the growing peptide oligomer (19), low concentrations of the FA monomer in plants can block possible sites for growth either on an esterified FA or on a protein-tyrosine template. High levels of FA statistically enhance dimerization to the decarboxylated FA dimers that enable further polymerization as established in the present study. The regulation of plant cell wall growth via control of the level of FA would therefore be amplified by an intrinsic feature of FA chemistry inevitably associated with FA concentration in the presence of peroxidases. We suggest that FA and possibly related cinnamic acid derivatives can exert two opposite effects on the growth of plant cell wall tissue, solely dependent on the incident concentration.

Acknowledgment—We are grateful to Richard Blaauw for helpful discussions.

REFERENCES

- Ostergaard, L., Teilum, K., Mirza, O., Mattsson, O., Petersen, M., Welinder, K. G., Mundy, J., Gajhede, M., and Henriksen, A. (2000) *Plant Mol. Biol.* **44**, 231–243
- Lewis, N. G., Yamamoto, E., Wooten, J. B., Just, G., Ohashi, H., and Towers, G. H. N. (1987) *Science* **237**, 1344–1346
- Nose, M., Bernards, M. A., Furlan, M., Zajicek, J., Eberhardt, T. L., and Lewis, N. G. (1995) *Phytochemistry* **39**, 71–79
- Bernards, M. A., and Razem, F. A. (2001) *Phytochemistry* **57**, 1115–1122
- Bernards, M. A., Lopez, M. L., Zajicek, J., and Lewis, N. G. (1995) *J. Biol. Chem.* **270**, 7382–7386
- Bunzel, M., Ralph, J., Marita, J. M., Hatfield, R. D., and Steinhart, H. (2001) *J. Sci. Food Agric.* **81**, 653–660
- Oosterveld, A., Pol, I. E., Beldman, G., and Voragen, A. G. J. (2001) *Carbohydr. Polym.* **44**, 9–17
- Henriksen, A., Smith, A. T., and Gajhede, M. (1999) *J. Biol. Chem.* **274**, 35005–35011
- Ralph, J., Helm, R. F., and Quideau, S. (1992) *J. Chem. Soc. Perkin Trans. I* **21**, 2971–2980
- Ralph, J., Helm, R. F., Quideau, S., and Hatfield, R. D. (1992) *J. Chem. Soc. Perkin Trans. I* **21**, 2961–2969
- Ralph, J. (1994) *J. Chem. Soc. Perkin Trans. I* **1**, 3485–3498
- Oosterveld, A., Grabber, J. H., Beldman, G., Ralph, J., and Voragen, A. G. J. (1997) *Carbohydr. Res.* **300**, 179–181
- Grabber, J. H., Ralph, J., and Hatfield, R. D. (2000) *J. Agric. Food Chem.* **48**, 6106–6113
- Oosterveld, A., Beldman, G., and Voragen, A. G. J. (2000) *Carbohydr. Res.* **328**, 199–207
- Ward, G., Hadar, Y., Bilkis, I., Konstantinovskiy, L., and Dosoretz, C. G. (2001) *J. Biol. Chem.* **276**, 18734–18741
- Gross, A. J., and Sizer, I. W. (1959) *J. Biol. Chem.* **234**, 1611–1614

17. Michon, T., Chenu, M., Kellershon, N., Desmadril, M., and Gueguen, J. (1997) *Biochemistry* **36**, 8504–8513
18. Wang, W., Noel, S., Desmadril, M., Gueguen, J., and Michon, T. (1999) *Biochem. J.* **340**, 329–336
19. Oudgenoeg, G., Hilhorst, R., Piersma, S. R., Boeriu, C. G., Gruppen, H., Hessing, M., Voragen, A. G. J., and Laane, C. (2001) *J. Agric. Food Chem.* **49**, 2503–2510
20. Andersen, S. O. (1964) *Biochim. Biophys. Acta* **93**, 213–216
21. Bradley, D. J., Kjellbom, P., and Lamb, C. J. (1992) *Cell* **70**, 21–30
22. Michon, T., Wang, W., Ferrasson, E., and Gueguen, J. (1999) *Biotechnol. Bioeng.* **63**, 449–458
23. Davin, L. B., and Lewis, N. G. (2000) *Plant Physiol.* **123**, 453–462
24. Gang, D. R., Costa, M. A., Fujita, M., Dinkova-Kostova, A. T., Wang, H. B., Burlat, V., Martin, W., Sarkanen, S., Davin, L. B., and Lewis, N. G. (1999) *Chem. Biol. (Lond.)* **6**, 143–151
25. Davin, L. B., Wang, H. B., Crowell, A. L., Bedgar, D. L., Martin, D. M., Sarkanen, S., and Lewis, N. G. (1997) *Science* **275**, 362–366

Horseradish Peroxidase-catalyzed Oligomerization of Ferulic Acid on a Template of a Tyrosine-containing Tripeptide

Gideon Oudgenoeg, Eef Dirksen, Steen Ingemann, Riet Hilhorst, Harry Gruppen, Carmen G. Boeriu, Sander R. Piersma, Willem J. H. van Berkel, Colja Laane and Alphons G. J. Voragen

J. Biol. Chem. 2002, 277:21332-21340.

doi: 10.1074/jbc.M201679200 originally published online March 29, 2002

Access the most updated version of this article at doi: [10.1074/jbc.M201679200](https://doi.org/10.1074/jbc.M201679200)

Alerts:

- [When this article is cited](#)
- [When a correction for this article is posted](#)

[Click here](#) to choose from all of JBC's e-mail alerts

This article cites 24 references, 7 of which can be accessed free at <http://www.jbc.org/content/277/24/21332.full.html#ref-list-1>